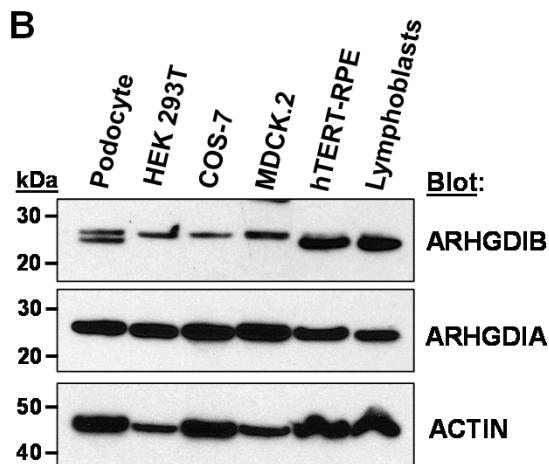
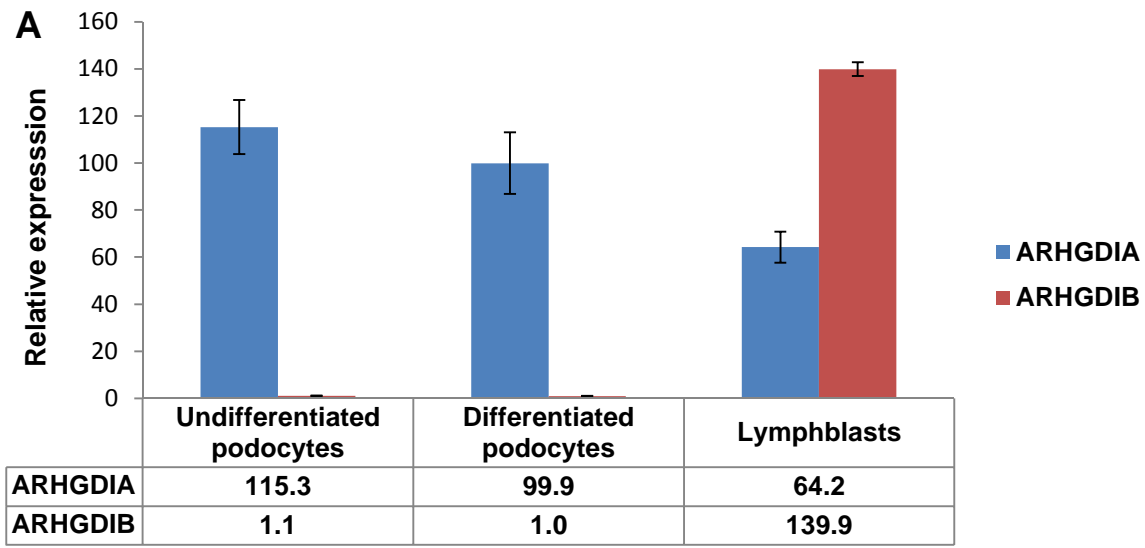
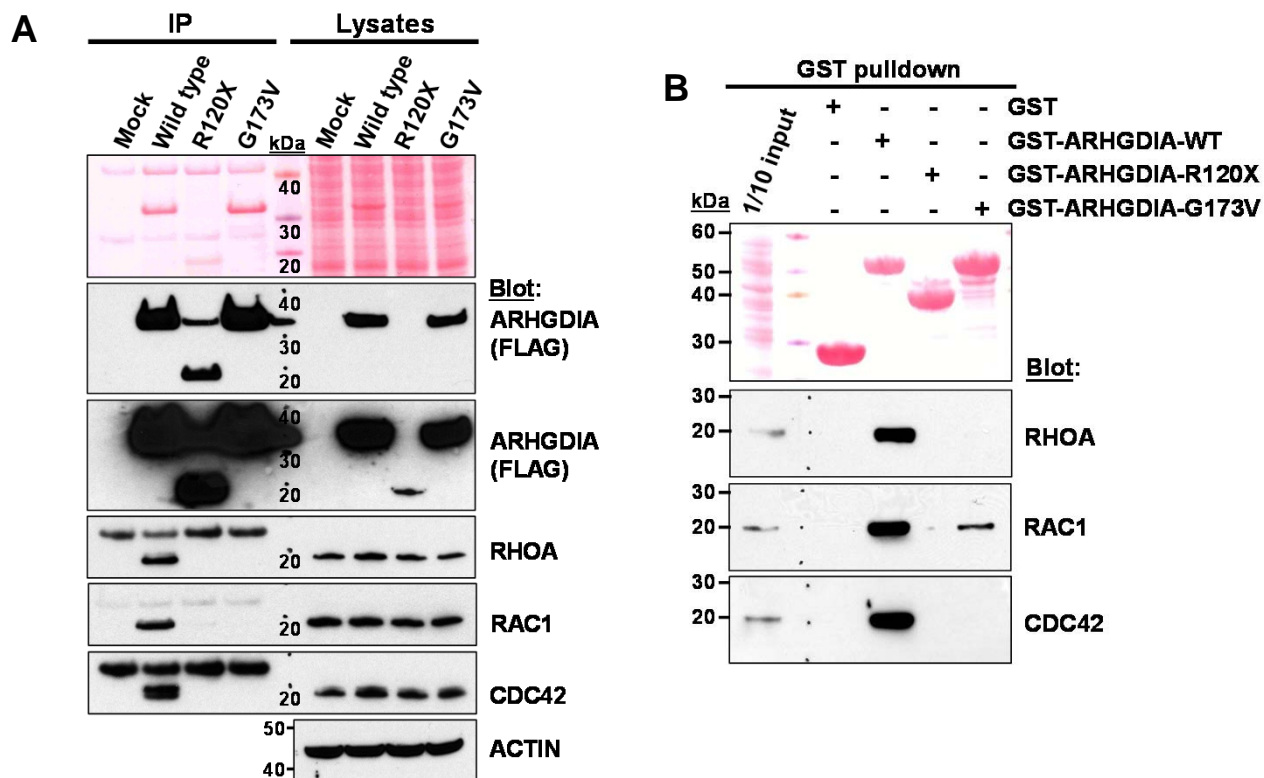


## Supplemental Figures



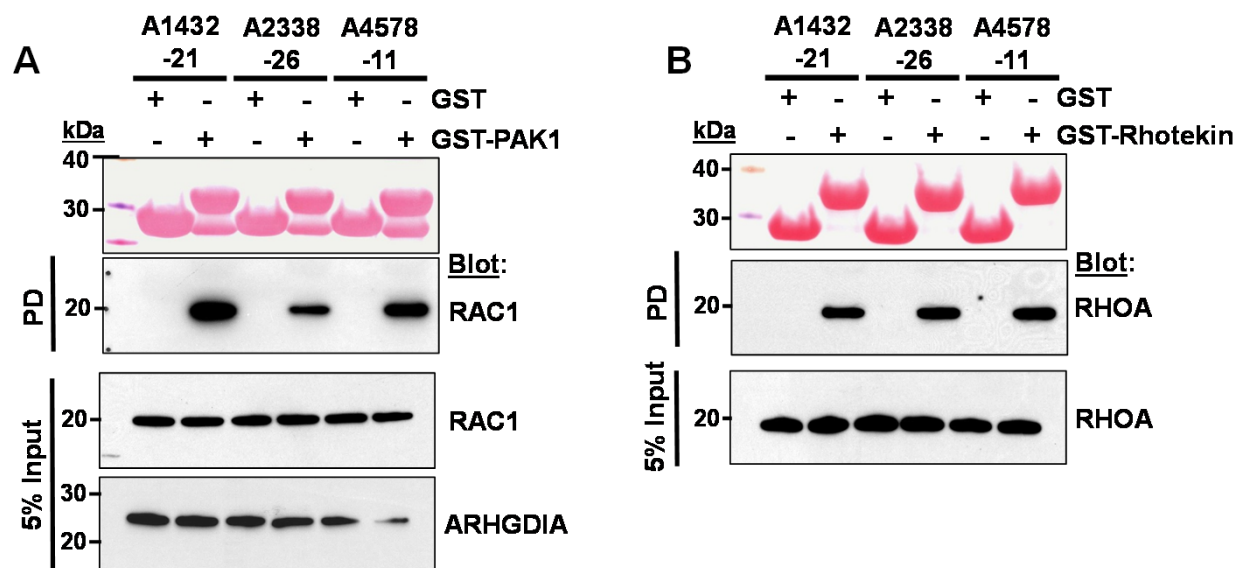
### Supplemental Figure 1. Differential expression of ARHGDI A and ARHGDI B in podocytes

**(A)** Expression measured by quantitative real-time PCR was normalized to GAPDH expression. Note that, whereas ARHGDI B is expressed more in lymphoblasts, ARHGDI A are 100 times more expressed in both undifferentiated and differentiated podocytes than ARHGDI B. Real-time PCR was performed using StepOnePlus™ Real-Time PCR System (Applied Biosystems). TaqMan probes for *ARHGDI A* (Hs00366348\_g1), *ARHGDI B* (Hs00171288\_m1), and *glyceraldehyde-3-phosphate dehydrogenase (GAPDH)* (Hs02758991\_g1) were purchased from Applied Biosystems. The relative RNA expression levels were calculated via a comparative threshold cycle (Ct) method using *GAPDH* as control:  $\Delta Ct = Ct(GAPDH) - Ct(ARHGDI A \text{ or } ARHGDI B)$ . The gene expression fold change, normalized to the *GAPDH* and relative to the control sample (*ARHGDI B* expression in the differentiated podocytes), was calculated as  $2^{-\Delta\Delta Ct}$ . Error bars, s.e.m. of six experiments. **(B)** Expression of ARHGDI A and ARHGDI B in various cell lines. ARHGDI B is more enriched in lymphoblasts, in contrast, ARHGDI A is expressed ubiquitously. ARHGDI B antibody was purchased from BD Pharmingen.



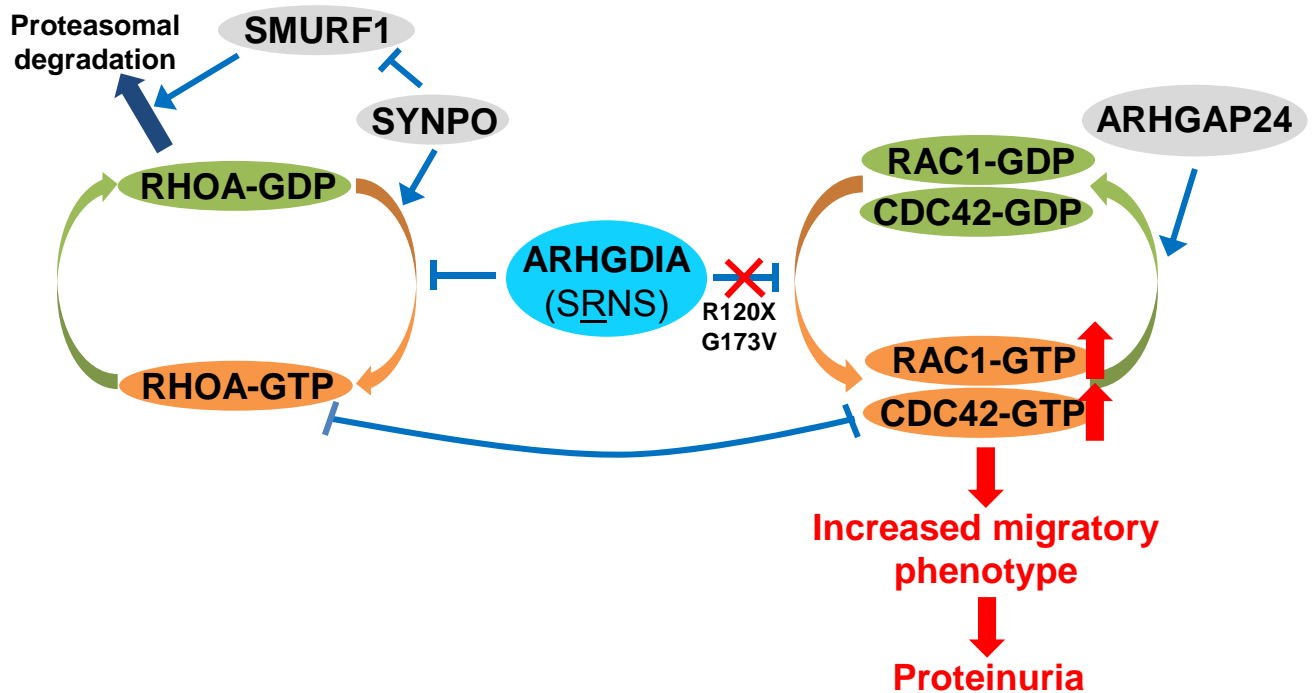
**Supplemental Figure 2. Interaction of ARHGDIA wild type (WT) and two mutants (p.R120X and p.G173V) with RHO GTPases in culture human podocytes.**

**(A)** Coimmunoprecipitation of FLAG-tagged ARHGDIA constructs with endogenous RHO GTPases. Coimmunoprecipitation were performed using anti-FLAG antibody and rec-Protein G-Sepharose 4B Conjugate (Invitrogen). **(B)** GST pulldown with purified ARHGDIA (WT and mutants) proteins. The GST proteins were incubated with lysates of differentiated human podocytes. This is the representative of more than 3 experiments. Note that R120X completely abrogates interaction with RHO GTPases. Compared to ARHGDIA WT, the mutant G173V abrogates interaction with RHOA and CDC42, and significantly decreased its interaction with RAC1. Data are congruent with the data from coimmunoprecipitation in **Figure 3A**.



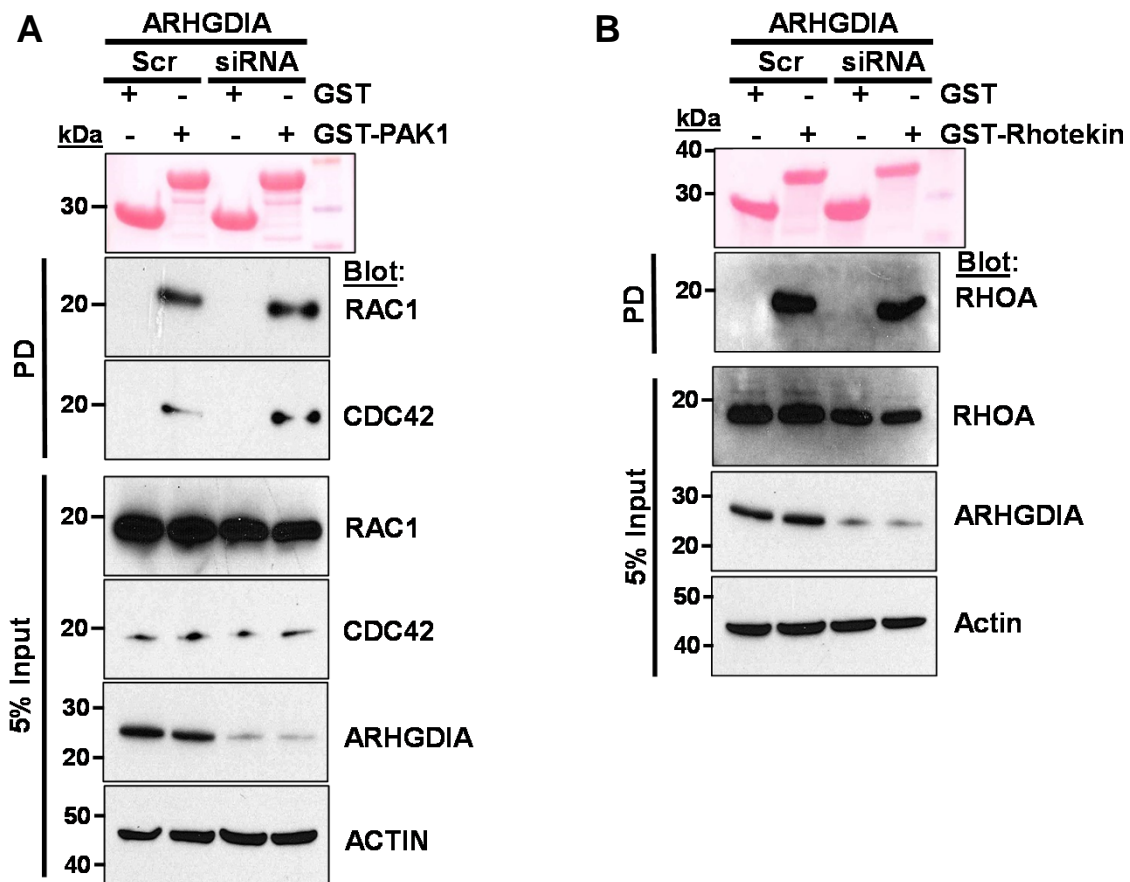
**Supplemental Figure 3. Effects of ARHGDI A mutations on RHO GTPase activity in Epstein-Barr virus (EBV)-transformed lymphoblasts.**

(A) Active GTP-bound RAC1 precipitated from EBV-transformed lymphocytes from a patient A1432-21 using GST-PAK1 (CRIB) pulldown assay. A1432-21 has DMS and has a homozygous mutation in *ARHGDI A* (G173V). A2338-26 is a healthy control. A4578-11 is the father of A4578-21, has a heterozygous *ARHGDI A* mutation (R120X) and thereby serves as a negative control. Lymphocytes derived from A1432-21 showed significant increase in relative RAC1 when compared to lymphocytes derived from A2338-26 or the heterozygous father A4578-11. GTP-bound CDC42 was not detected in lymphocytes of patients or controls (data not shown). (B) Active GTP-bound RHOA precipitated from EBV-transformed lymphocytes In the individuals tested there was no significant difference in the lymphocyte levels of GTP-bound RHOA. PD denotes pulldown.



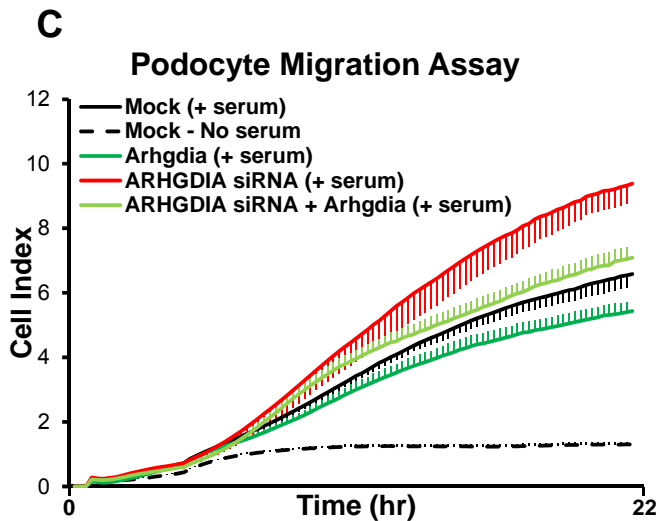
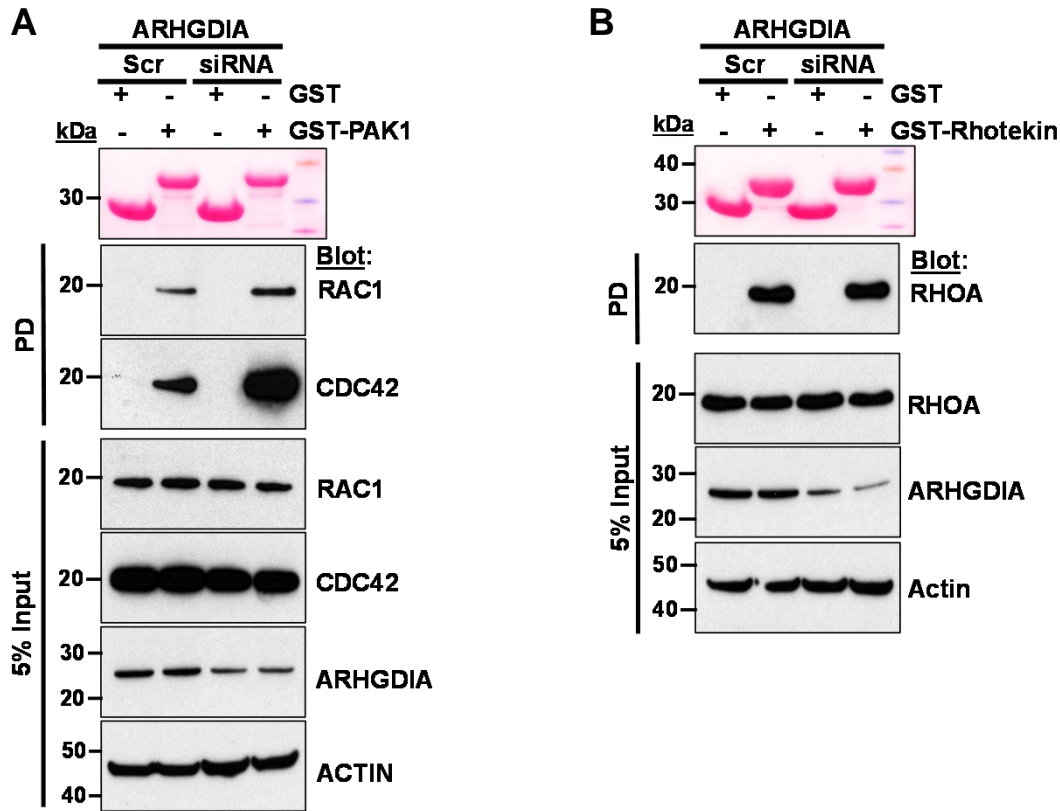
**Supplemental Figure 4. Schematic showing the pathomechanisms of RHO small GTPase signaling in nephrotic syndrome caused by mutations in *ARHGDI A*.**

Both *ARHGDI A* mutations (R120X and G173V) detected in families (A1432 and A4578) with SRNS abrogate interaction with RHO GTPases, increase active GTP-bound RAC1 and CDC42, but not RHOA, and result in an *increased migratory* podocyte phenotype, most likely causing podocyte foot process effacement and proteinuria. The roles of synaptopodin and smurf1 in RHOA regulation are also shown (32).



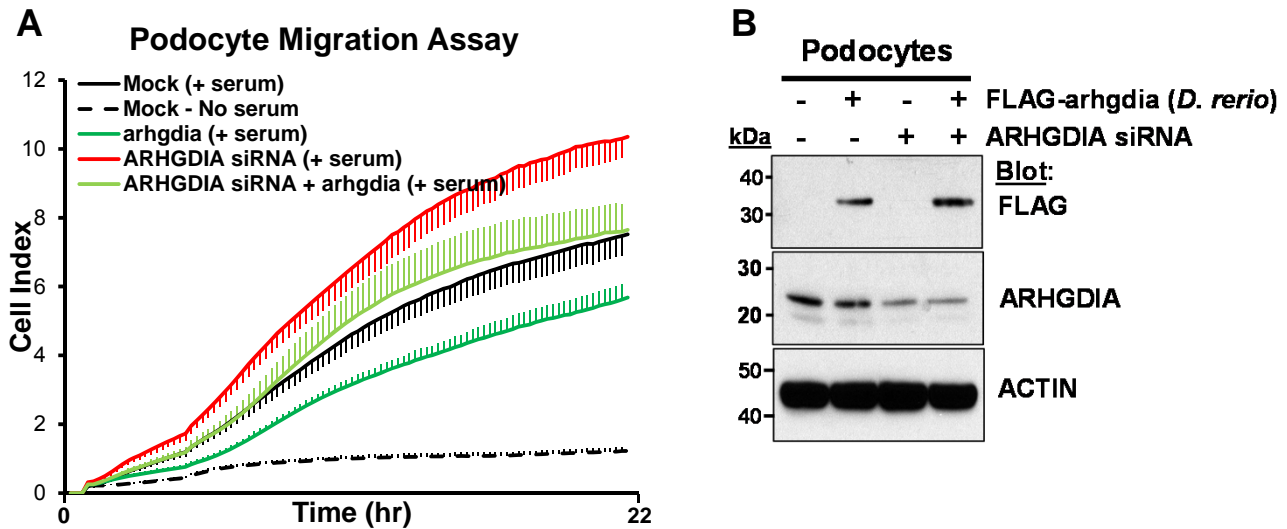
**Supplemental Figure 5. Effects of ARHGDI A knockdown on RHO GTPase activity in cultured human podocytes.**

This experiment was performed using *ARHGDI A* siRNA purchased from Sigma. **(A)** Active GTP-bound RAC1 and CDC42 precipitated from cultured human podocytes transfected with scrambled (Scr) or *ARHGDI A* siRNA using a GST-PAK1 (CRIB) pull-down assay. Compare to Scr control podocytes, podocytes transfected with siRNA knockdown of ARHGDI A exhibited an increase in relative RAC1 and CDC42 activity compared to podocytes transfected with scrambled siRNA. The efficiency of knockdown by siRNA was confirmed by immunoblotting with an anti-ARHGDI A antibody (second to lowest panel). **(B)** Active GTP-bound RHOA precipitated from podocytes transfected with scrambled or *ARHGDI A* siRNA using a GST-Rhotekin (RBD) pull-down assay. Cells transfected with scrambled control siRNA vs. *ARHGDI A* siRNA exhibited no significant difference in relative RHOA activity. Figures A and B are representative of 2 experiments each. PD denotes pull-down.



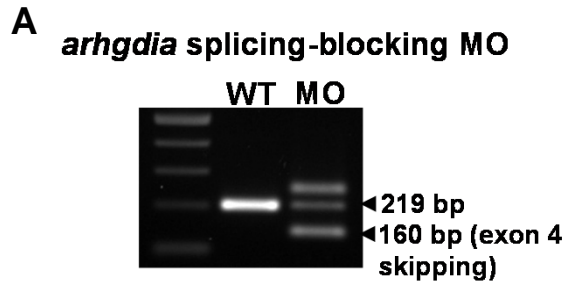
**Supplemental Figure 6. Effects of ARHG DIA knockdown on RHO GTPase activity and podocyte migration in cultured human podocytes.**

This experiment was performed using *ARHG DIA* siRNA which was previously described (41). **(A)** Active GTP-bound RAC1 and CDC42 precipitated by a GST-PAK1 (CRIB) pull-down assay. **(B)** Active GTP-bound RHOA precipitated by GST-Rhotekin (RBD) pull-down assay. Figures A and B are representative of 2 experiments each. PD denotes pull-down. **(C)** The effect of *ARHG DIA* knockdown on podocyte migration. Podocytes transfected with *ARHG DIA* siRNA exhibited more active migration compared to podocytes transfected with scrambled siRNA control. The increase in podocyte migration by *ARHG DIA* knockdown (red) was rescued by transfection of mouse *Arhgdia* into podocytes (light green). Mouse *Arhgdia* has two base mismatches from the siRNA target sequences. Note that overexpression of mouse *Arhgdia* inhibited podocyte migration (green). Error bars are shown in only one direction for clarity and indicate standard deviations for >4 independent experiments.



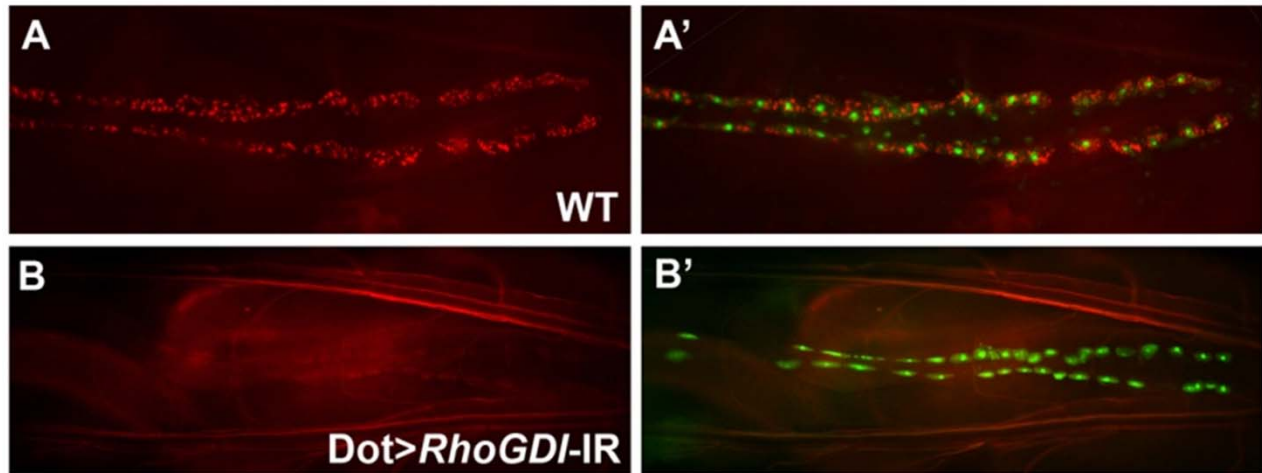
**Supplemental Figure 7. Rescue of the increased migratory phenotype of podocytes induced by ARHGDIA knockdown.**

The *ARHGDIA* siRNA was also used in **Supplemental Figure 5**. **(A)** Podocytes transfected with *ARHGDIA* siRNA (red) exhibited more active migration compared to podocytes transfected with scrambled siRNA control (black). The increase in podocyte migration by *ARHGDIA* knockdown (red) was rescued by transfection of zebrafish *arhgdia* into podocytes (light green). Zebrafish *arhgdia* has two base mismatches from the siRNA target sequences. Note that overexpression of zebrafish *arhgdia* inhibited podocyte migration (green). Error bars are shown in only one direction for clarity and indicate standard deviations for >4 independent experiments. **(B)** Podocytes were transfected with scrambled or *ARHGDIA* siRNA, and with FLAG-tagged *arhgdia* (*D. rerio*) or mock plasmid. Western blot showed that *ARHGDIA* siRNA which target the human ARHGDIA did not affect zebrafish *arhgdia*.



**Supplemental Figure 8. *arhgdia* knockdown by a splicing-blocking MO in zebrafish**

**(A)** RT-PCR was performed to detect the transcript of *arhgdia* in 48 hpf embryos. In embryos (WT) injected with 0.2 mM of negative control MO targeting *p53* (to control for unspecific apoptosis effects) (36) only the normal splicing product (219 bp) appeared. In contrast, in embryos (MO) injected with 0.2 mM MO targeting the acceptor site of intron 3 of *arhgdia*, a spliced product of 160 bp was detected that lacked exon 4 as confirmed by direct sequencing of the RT-PCR product. **(B-C)** Zebrafish coinjected with a splicing-blocking MO and with *p53* MO. At 120 hpf, *arhgdia* morphants displayed phenotype of periorbital edema (arrows) and total body edema in 64 % of embryos (104/163). Scale bars 1 mm in A and B.



**Supplemental Figure 9. *RhoGDI*, the *Drosophila* homologue of *ARHGDI*, is required for pericardial nephrocyte function.**

**(A-B)** RNAi knockdown of *RhoGDI* (**B**) dramatically reduced ANG-RFP (red) uptakes. A'-B' show the same larvae as A-B with Hand-GFP (green) labeling the pericardial nephrocytes (green). The *Drosophila* nephrocytes share remarkable similarities to the glomerular podocytes, making it a potent animal system to identify and study genes involved in podocyte biology (38). From a functional genetic screen for *Drosophila* pericardial nephrocyte (38), we identified the *Drosophila* ortholog of human *ARHGDI*. Pericardial nephrocyte specific knockdown of *Drosophila RhoGDI* (CG7823) dramatically reduced the ability of secreted protein uptake, a functional readout for pericardial nephrocytes in *Drosophila*, suggesting that *RhoGDI* is required for nephrocyte function.

Supplemental Table 1. Filtering process for variants from normal reference sequence (VRS) following whole exome resequencing in family A1432 with nephrotic syndrome

FAMILY	AFFECTED SIBS SENT FOR WER	Consanguinity	# of homozygosity peaks	Total homozygosity [Mb]	Total sequence reads (Mill.)	Matched Reads	Total DIPs	Exonic DIPs	% exonic / total DIPs	DIPs which are not SNP129	DIPs in linked region	DIPs after inspection and which are not SNP132 (>1%)	Sanger confirmation / Segregation	Total SNPs	Exonic SNPs	% exonic / total SNPs	SNPs which are not SNP129	SNPs in linked region	SNPs after inspection and which are not SNP132 (>1%)	Sanger confirmation / Segregation	Causative gene	Mutation effect on gene product	Comments
A1432	A1432-21	Y	5	108	66	87.2%	188,242	488	0.30%	317	96	3	0	354,041	5,900	1.70%	551	79	24	3	ARDHGIA	G173V (H)	The 3 remaining mutations in 3 different genes that were confirmed by Sanger sequencing and segregated with the affected status of the family were ARHGDIS <sup>d</sup> (G173V, H); KRT83 <sup>e</sup> (E201X, H) and TOM1L2 <sup>f</sup> (E458D, H).

<sup>a</sup>see Table 1

<sup>b</sup>see Figure 1

<sup>c</sup>Red numbers denote number of filtered-down variants that contained the disease causing gene.

<sup>d</sup>ARDHGDIS is most likely the causative gene as Arhgdia<sup>-/-</sup> mice developed massive proteinuria at 12 weeks of age and prematurely died of renal failure.

Kidney histology shows mesangial sclerosis and cystic tubular dilation (30).

<sup>e</sup>KRT83 or Keratin, hair basic 3 gene is known to cause Monilethrix.

<sup>f</sup>Missense mutation found in TOM1L2 gene is only conserved to Danio rerio.

"-" , not applicable; WER, whole exome resequencing; DIP, deletion/insertion polymorphism; SNP, single nucleotide polymorphism; Y, yes; (>1%), the allele frequency is greater than 1% in population.